Identification of Residues in the Monocyte Chemotactic Protein-1 That Contact the MCP-1 Receptor, CCR2†

Stefan Hemmerich,‡ Chad Paavola,§ Adam Bloom,§ Sunil Bhakta,‡ Richard Freedman,‡,|| Dorit Grunberger,‡ John Krstenansky,‡,⊥ Simon Lee,‡ Debbie McCarley,‡ Mary Mulkins,‡ Belinda Wong,‡ Joe Pease,‡ Laura Mizoue,§ Tara Mirzadegan,‡ Irene Polsky,‡ Kelly Thompson,‡ Tracy M. Handel,*,§ and Kurt Jarnagin*,‡,@

Department of Molecular and Cell Biology, University of California at Berkeley, Berkeley, California 94720, and Roche Bioscience, 3401 Hillview Avenue, Palo Alto, California 94304

Received May 5, 1999; Revised Manuscript Received July 28, 1999

ABSTRACT: The CC chemokine, MCP-1, has been identified as a major chemoattractant for T cells and monocytes, and plays a significant role in the pathology of inflammatory diseases. To identify the regions of MCP-1 that contact its receptor, CCR2, we substituted all surface-exposed residues with alanine. Some residues were also mutated to other amino acids to identify the importance of charge, hydrophobicity, or aromaticity at specific positions. The binding affinity of each mutant for CCR2 was assayed with THP-1 and CCR2-transfected CHL cells. The majority of point mutations had no effect. Residues at the N-terminus of the protein, known to be crucial for signaling, contribute less than a factor of 10 to the binding affinity. However, two clusters of primarily basic residues (R24, K35, K38, K49, and Y13), separated by a 35 Å hydrophobic groove, reduced the level of binding by 15−100-fold. A peptide fragment encompassing residues 13−35 recapitulated some of the mutational data derived from the intact protein. It exhibited modest binding as a linear peptide and dramatically improved affinity when the region which adopts a single turn of a 3^{10}-helix in the protein, which includes R24, was constrained by a disulfide bond. Additional constraints at the ends of the peptide, corresponding to the disulfide between the first and third cysteines in MCP-1, yielded further improvements in affinity. Together, these data suggest a model in which a large surface area of MCP-1 contacts the receptor, and the accumulation of a number of weak interactions results in the 35 pM affinity observed for the wild-type (WT) protein. The receptor binding site of MCP-1 also is significantly different from the binding sites of RANTES and IL-8, providing insight into the issue of receptor specificity. It was previously shown that the N-terminus of CCR2 is critical for binding MCP-1 [Monteclaro, F. S., and Charo, I. F. (1996) *J. Biol. Chem. 271*, 19084−92; Monteclaro, F. S., and Charo, I. F. (1997) *J. Biol. Chem. 272*, 23186−90]. Point mutations of six acidic residues in this region of the receptor were made to test their role in ligand binding. This identified D25 and D27 of the DYDY motif as being important. On the basis of our data, we propose a model in which the receptor N-terminus lies along the hydrophobic groove in an extended fashion, placing the DYDY motif near the basic cluster involving R24 and K49 of MCP-1. This in turn orients the signaling residues (Y13 and the N-terminus) for productive interaction with the receptor.

Chemokines are small proteins most noted for their ability to recruit leukocytes to sites of inflammation (*3*−*7*), although there is some speculation that they may also be involved in other developmental processes that exploit their ability to control cell migration (*8*). These proteins have been classified into four subfamilies based on the chromosomal location of their genes and the pattern of cysteine residues which form structurally important disulfide bonds. The two major families are the α/CXC chemokines which chemotax neutrophils and nonhematopoietic cells and the β/CC chemokines which recruit monocytes, T cells, eosinophils, and NK cells. The only known C-chemokine, lymphotactin, is a T and NK cell chemoattractant (*9*), while fractalkine/neurotactin, a CX_3C chemokine, attracts T cells, monocytes, and NK cells (*8*, *10*).

Among the CC chemokines, the monocyte chemoattractant protein-1 (MCP-1) has received a great deal of attention because of its in vivo role as a monocyte and T cell chemoattractant (*11*−*14*) and its purported involvement in a number of inflammatory diseases (*15*). Several studies have shown that the level of MCP-1 expression is elevated in the inflamed synovium of patients with rheumatoid arthritis, but can be reduced by antiarthritic drugs (*16*−*20*). It is also

† This work was supported by grants awarded to T.M.H. by the National Institutes of Health, the American Heart Association, and the Pew Scholars Program in the Biomedical Sciences.

* To whom correspondence should be addressed. T.M.H.: phone, (510) 643-9313; fax, (510) 643-9290; e-mail, handel@paradise1.berkeley.edu. K.J.: phone, (650) 567-5503; fax, (650) 562-3034; e-mail, kjarnagin@iconixpharm.com.

‡ Roche Bioscience.

§ University of California at Berkeley.

|| Current address: Hyseq Inc., 670 Alomar Ave., Sunnyvale, CA 94086.

⊥ Current address: EnzyMed Inc., 2501 Crosspark Rd., Suite C-150, Iowa City, IA 52242.

@ Current address: Iconix Pharmaceuticals, 850 Maude Ave., Mountain View, CA 94043.

10.1021/bi991029m CCC: $18.00
Published on Web 09/15/1999

elevated in asthmatic patients where the level of expression correlates with the severity of symptoms, but can be suppressed by immunotherapy (*21*−*24*). Finally, high levels are found in the atherosclerotic lesions of humans, and cholesterol-fed rabbits (*25*, *26*). Treatment with MCP-1 neutralizing antibodies or other biological antagonists reduced inflammation in a number of animal models, including lung granuloma (*27*, *28*), lipopolysacharride-induced death (*29*), glomerulonephritis (*30*), delayed-type hypersensitivity in the skin (*31*), and adjuvant arthritis in mice (*32*). These findings and knockouts of either MCP-1 or its receptor CCR2 (*33*−*35*) demonstrate that modulation of MCP-1 expression or activity may be beneficial in treating inflammatory diseases and atherosclerosis. This has encouraged significant efforts to understand the mechanistic details of how MCP-1 binds its seven transmembrane G-protein-coupled receptor, CCR2, and to develop reagents to interfere with the interaction.

In the study presented here, we identified surface-exposed residues of MCP-1 which are important for binding to CCR2. Our results refine and extend conclusions from related studies (*36*−*40*) by providing a comprehensive analysis of the receptor binding site with a series of 58 mutants. We also explore the role of the amino terminus of MCP-1 with alanine scanning mutagenesis rather than truncation to complement previous work that implicates this region as being critical for binding and agonism (*36*, *39*). Finally, we analyzed the effect of mutations of acidic residues in the N-terminus of CCR2. Together, these data allow us to construct a preliminary low-resolution model of the interaction between MCP-1 and CCR2, which can be used to guide future mutagenesis studies of the receptor. Comparison of our results to mutagenesis studies with IL-8[1] and RANTES also provides insight into the structural basis for chemokine−receptor specificity.

MATERIALS AND METHODS

Preparation of MCP-1 Mutants. Gene construction, expression, and purification of WT and mutant MCP-1, including ^{15}N-labeled protein, were carried out as previously reported (*41*).

Synthesis, Oxidation, and Purification of Peptides. Peptides were synthesized by Multiple Peptide Systems (San Diego, CA). Single disulfide formation was achieved by iodine oxidation of peptides in a solution containing acetic acid (*42*). Regioselective formation of double-disulfide bridges was achieved using two orthogonally removable sets of paired cysteine-protecting groups, trityl and methoxybenzyl. After synthesis of peptides using traditional Fmoc-tButyl chemistry, the trityl groups were removed from the cysteines concurrent with cleavage from the resin using reagent K, a mixture of TFA, phenol, water, thioanisole, and ethanedithiol (*43*). Crude peptides were oxidized in solution with iodine and purified by preparative reversed-phase HPLC (RP-HPLC). The methoxybenzyl groups were then removed and the peptides simultaneously oxidized using 10% DMSO and 2% anisole in TFA (*44*). Each peptide was characterized by RP-HPLC for purity, which typically exceeded 95%. The molecular mass of each peptide was determined using a SCIEX API 1 electrospray mass spectrometer or a Bio-Ion 20 Plasma Desorption mass spectrometer. All masses were within ±0.5 Da of the expected values.

Preparation, Isolation, and Characterization of L1.2 Transfectants Bearing the Mutant Receptor. Receptor mutations were introduced into pcDNA3.1 containing an amino-terminal flag tagged hCCR2 receptor (*1*) using a previously reported PCR method (*45*). This method amplifies the region of receptor immediately surrounding the target mutation site. The region amplified during the mutagenesis procedure was sequenced to confirm the presence of the mutation and the absence of unintended mutations.

Mutant and wild-type receptor-bearing plasmids were transfected into L1.2 cells, an Abelson virus transformed mouse B cell line obtained as a gift from E. Butcher. Transfection and isolation of L1.2 cells lines were carried out with lipofectamine and procedures similar to those previously described (*45*). Transfected L1.2 cells were treated with 2 mM sodium butyrate in RPMI medium at a density of 1×10^5 cells/mL for 5.5 h to increase the level of cell surface expression of the receptor. The treatment was performed prior to all receptor quantitation, affinity determinations, and cell cloning procedures. The level of cell surface receptor expression was increased 6.9-fold, as measured by epitope tag specific fluorescent antibody staining. Accordingly, the level of MCP-1 binding increased 4.1-fold (from 5100 to 21 000 receptors/cell).

Fluorescence-activated cell sorting was used to isolate single clones and to quantify receptor expression. For flow cytometry, 5×10^5 cells were stained with 1 μg of anti-flag M1 monoclonal antibody (Eastman Kodak, New Haven, CT) followed by 5.6 μg of FITC-conjugated goat antibody. The mean fluorescent intensity of receptor-bearing cell lines compared to that of untransfected L1.2 cell controls was used as a semiquantitative measure of the level of receptor expression. This ratio correlates with the level of receptor expression as measured by radiolabeled ligand receptor binding assays (see the sodium butyrate treatment above). Upon isolation, clones were checked to confirm the presence of DNA encoding the desired mutation. Genomic DNA from the clone was isolated using a QIAamp blood DNA isolation kit (Qiagen GmbH, Hilden, Germany). The genomic DNA was used as the template for PCR using primers encoded by the T7 region of the pCDNA3.1 vector and a 3′-primer within the receptor coding region, 5′-TAGAAGGCACAGTCGAGG. The PCR products were purified using Geneclean columns (Bio101, La Jolla, CA) and then sequenced.

Binding Assay. Membranes were prepared from cells that were washed in phosphate-buffered saline and resuspended in a 5-fold dilution of MCP buffer with protease inhibitors and 0.2 mM EDTA. The cells were homogenized using five strokes of a Dounce homogenizer followed by sonication; each 25 mL aliquot was sonicated twice for 15 s at the maximum level that does not cause foaming. DNAse was added to a final concentration of 20 μg/mL, and the homogenate was rocked for 10 min at room temperature. The cell debris was removed by centrifugation at 500*g* for 5 min. Membranes were then pelleted by centrifuging the

[1] Abbreviations: HSQC, heteronuclear single-quantum correlation experiment; hMCP-1, human MCP-1; mMCP-1, mouse MCP-1; [1+9−76]hMCP-1, hMCP-1 with residues 2−8 deleted; [1+10−76,7/9]hMCP-1, hMCP-1 with residues 2−9 deleted and seven of nine lysines changed to arginine or methionine (K75 and K69 are retained); WT*, hMCP-1 with a mutation of M64I; MGSA, melanoma growth stimulating activity; IL-8, interleukin-8; RANTES, regulated upon activation, normal T cell-expressed, and secreted; TFA, trifluoroacetic acid; GPCR, G-protein-coupled receptor; TM-7, transmembrane helix 7.

supernatant for 30 min at 48000*g*. Finally, the membrane pellet was resuspended in binding buffer. MCP buffer consists of 50 mM HEPES (pH 7.2), 1 mM $CaCl_2$, 5 mM $MgCl_2$, and 0.1% BSA. Protease inhibitors include 0.1 mM PMSF, 1 μM leupeptin, and 0.35 μg/mL pepstatin.

The level of binding of MCP-1 mutants was measured using membranes prepared from two cell lines, THP-1 and CCR2-CHL. For the peptides, binding was only tested in CCR2-CHL cells. Each 300 μL assay was composed of membranes from 1×10^6 THP-1 cells or 0.5×10^6 CCR2-CHL cells, 50 pM [^{125}I]MCP (NEN Life Science Products, Bedford, MA) at 1100 or 550 Ci/mmol, MCP buffer, protease inhibitors, and test protein or peptide. Equilibrium was achieved by incubation at 28 °C for 90 min. Membrane-bound [^{125}I]MCP was collected by filtration through GF/B filters presoaked in 0.3% polyethyleneimine and 0.05% BSA, followed by four rapid washes with approximately 0.5 mL of ice cold buffer containing 0.5 M NaCl and 10 mM HEPES (pH 7.4).

THP-1 cells are a human monocyte cell line (ATCC TIP-202) that express both CCR1 and CCR2. CCR2-CHL cells are Chinese hamster lung cells (ATCC CRL-1657) that have been stably transformed with an expression vector, pSW104, bearing the human CCR2b receptor and a neomycin resistance marker plasmid as previously described (*45*). The CCR2-CHL and the THP-1-4X cells express approximately 10 000 CCR2 receptors per cell, while THP-1, HEK-293-CCR2b, and CHO-K1-CCR2b-cAMP-Luc-neo-22 cells express approximately 5000 CCR2 receptors/cell (see below).

NMR. One-dimensional proton spectra were collected with a standard presaturation experiment to attenuate the water signal. Two-dimensional ^{1}H−^{15}N HSQC spectra were recorded with a program that uses gradients and water flipback pulses (*46*) on a Bruker DMX spectrometer at 35 °C. Samples were approximately 1 mM at pH 5.40. The ^{1}H and ^{15}N spectral widths were 8090.615 and 800 Hz, respectively, with sign discrimination of aliased cross-peaks in the ^{15}N dimension. One hundred twenty-eight complex pairs were recorded for a total acquisition time in the indirect dimension of 160 ms. Data were processed with the program Azara (W. Boucher, unpublished results) by zero-filling once and apodizing with a squared sine-bell function in the direct and indirect dimensions. Chemical shifts were referenced indirectly to 2,2-dimethyl-2-silapentane-5-sulfonate (DSS) at 25 °C using 3-(trimethylsilyl)propionate (TSP) to calibrate the temperature (*47*).

Modeling of CCR2. The model for CCR2 (Figure 8) was generated as follows. Sequence alignment of more than 100 GPCRs was used to identify the hydrophobic transmembrane regions of the human CCR2 receptor. A model of rhodopsin based on the bacteriorhodopsin structure was used as a template, and the appropriate residues of the helices were mutated to the corresponding amino acid from the sequence alignment using the program INSIGHTII (Molecular Simulations, San Diego, CA). The side chains were minimized and placed in a reasonable conformation. The helices were connected with appropriate loops; however, the conformations of the loops are meaningless.

RESULTS

Mutagenesis Strategy. The surface-exposed residues of MCP-1 were identified with GRASP1.1 (*48*) by computing the solvent accessible surface area (SASA) from a monomer subunit of the experimentally determined structures (*49*, *50*). The maximum solvent accessible surface area for each amino acid was estimated utilizing GGXGG model peptides. Using a PCR-based strategy, we mutated all residues with a SASA of >33%, except for residues at the C-terminus which are known to be unimportant for binding (*37*). Most mutants were made in the context of MCP-1 M64I, termed WT*, which behaves just like WT in binding and activity assays (*41*). Initially, the chosen residues were individually changed to alanine. Charged or hydrophobic residues which altered binding were subsequently mutated to other residues to elucidate the importance of the chemical nature of the side chain. In total, 58 mutants were constructed, expressed, and purified. The average purity level was 95% based on analytical HPLC.

Binding of MCP-1 Mutants to THP-1 versus CCR2-CHL Cells. The binding affinity of each of the 58 mutants was measured with two cell types, THP-1 cells and CCR2-transfected Chinese hamster lung cells (CCR2-CHL). Both cell lines were used to assess the effect of cell background on binding and ensure that measurement of THP-1 affinities was not complicated by the presence of CCR1 receptors. The affinity of MIP-1α in the THP-1 assay is >100 nM, while MCP-1, MCP-2, and MCP-3 compete with K_d values of 35, 320, and 50 pM, respectively. This indicates that we only measure binding to CCR2 in the THP-1 assay. Figure 1 shows representative binding isotherms for WT MCP-1 and several of the mutants on THP-1 cells. As shown in Figure 2, the binding affinities of wild-type and mutant proteins were similar for THP-1 and CCR2-CHL cells (correlation coefficient of 0.98, slope of 0.95), also indicating that cell background does not influence the results. Figure 3 summarizes the binding data graphically for all the mutants, some of which are described in detail below. A complete table of the binding data, including replicate statistics, is available as Supporting Information.

Binding Data Reveal a Number of Important Residues That Are Distributed over a Large Surface of the Protein. Structural studies have revealed that most chemokines form homodimers at micromolar to millimolar concentrations (*49*−*54*). As part of an effort to determine whether MCP-1 binds and activates CCR2 as a monomer or dimer, we previously showed that alanine substitution of Y13, a residue critical to formation of the dimer, had a significant effect on binding and activity (*41*). In the work presented here, we have a more extensive set of mutants, but of all of the alanine mutants, Y13A had the largest effect on binding with a loss in affinity of 2 orders of magnitude relative to that of WT (Figure 3). Alignment of MCP-1 sequences from different species (Figure 4) indicates that Y13 is completely conserved. Mutation to Phe, an alternative residue found in other CC chemokines, does not affect binding. Mutation to larger (Trp) or more polar aromatics (His) or replacement with Leu reduced the level of binding by a factor of 4−22, defining some of the chemical requirements at this position. Others have shown a slightly reduced affinity with mutation to Ile, consistent with these results (*38*). Figure 5a shows a ribbon diagram illustrating the location of Y13 and other residues described below that produce the largest changes when mutated.

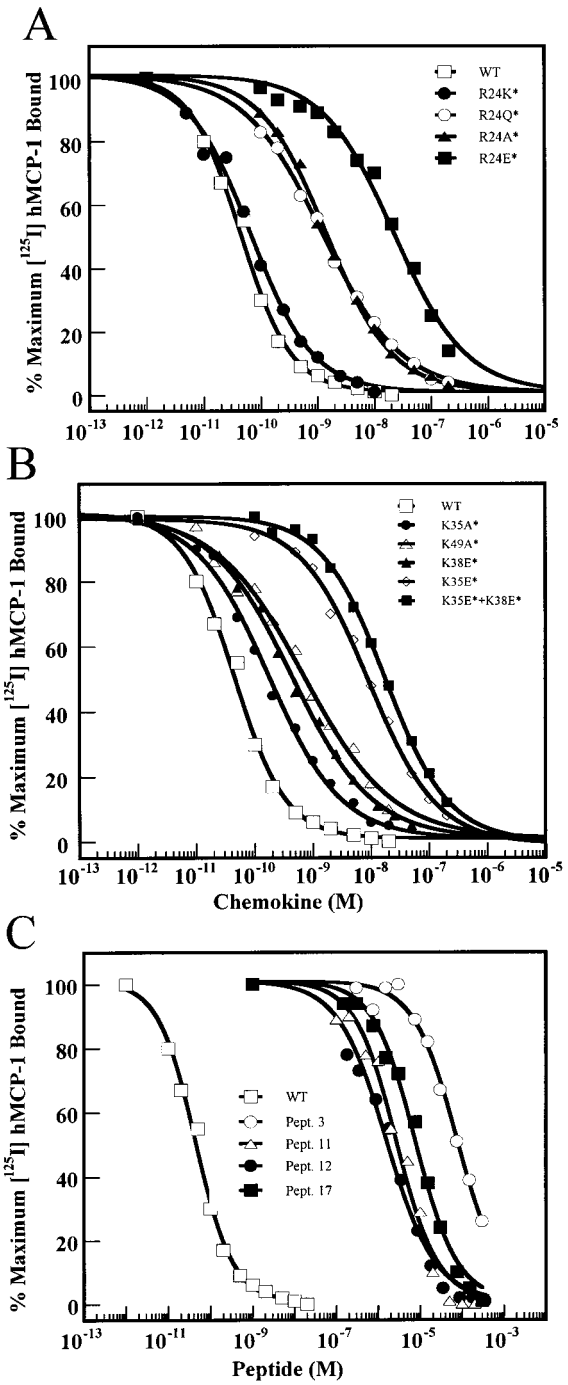

FIGURE 1: Displacement of [^{125}I]MCP-1 from CCR2 expressed on THP-1 cells (A and B) by unlabeled WT* and several MCP-1 mutants and (C) by peptide fragments of MCP-1. The data shown are representative of 2−11 experiments where each data point is the mean of duplicate measurements.

Additional residues which form part of the dimerization interface include V9 and T10. Single- and double-alanine mutants (V9A and V9A/T10A) had almost no effect on binding. However, mutation to Glu exaggerated the effects and resulted in a 6−30-fold loss of affinity, similar to previous reports of a T10 mutation to Arg (*38*). Like Y13, T10 is completely conserved among MCP-1 sequences from different species as well as in MCP-1−4 (Figure 4).

Of the alanine mutants, R24A had the second largest impact on binding (35-fold decrease in affinity, Figure 3). This residue is at the opposite end of the protein from Y13

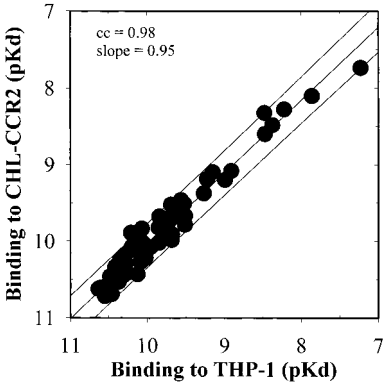

FIGURE 2: Correlation between the level of binding of the various mutants to CCR2 on THP-1 cells and CCR2-transfected CHL cells. Each data point is an average of between 2 and 441 separate determinations in each cell line using the mutants listed in Figure 3. The center line represents the best linear fit to the data, and the outer lines represent the 95% prediction confidence limits for the fit.

(Figure 5a) and is part of a 3^{10}-helix that is present in every chemokine structure that has been determined to date. It is conserved across different species of MCP-1 as well as in human MCP-2−4, but varies widely in other CC chemokines and therefore may be involved in receptor specificity. Mutation of R24 to Lys resulted in a protein with WT affinity. Mutation to Glu or Gln caused a 1600- and 28-fold reduction in the level of binding to THP-1 cells, respectively, suggesting that it interacts with a negatively charged residue of the receptor.

Residue 49 is conserved as a basic Arg or Lys in different MCP-1 species as well as most other CC chemokines (Figure 4). This residue is close to R24 (Figure 5a) on the same face of the protein. Mutation of K49 to Ala resulted in a 14−15-fold decrease in binding affinity. Replacement with an acidic residue has not yet been done to assess whether it is involved in electrostatic interactions with the receptor.

In the 30's loop which is held in proximity to Y13 via the disulfide bridge between C11 and C36, mutation of several residues to Ala had small (<10-fold) but measurable effects on binding. This includes K35 and K38 which are largely conserved as basic residues in different MCP-1 species, and P37 which is completely conserved in MCPs but predominantly Ser in other CC chemokines (Figure 4). Mutation of K35 to Glu caused a much greater reduction in affinity (169−175-fold), indicating that this residue may be involved in electrostatic interactions with the receptor, while K38E was only marginally worse then K38A. The double mutation (K35E/K38E) showed a 200−400-fold change in binding affinity which is what one would anticipate from the single mutations if the effects were additive (*55*). Insertion of a Pro between S34 and K35 reduced the binding affinity by more than 2 orders of magnitude, consistent with previous reports (*40*). Since Ala mutations of other residues in the loop have no or smaller consequences, we suspect that the effect of the Pro insertion is to change the orientation of key residues (Y13 and the N-terminus) which are structurally coupled to the 30's loop (see the NMR section below).

Much more modest effects were observed for several other residues. In the so-called N-loop which corresponds to residues between the first two cysteines and the 3^{10}-helix, R18A and K19A showed a 2−3-fold decrease in binding

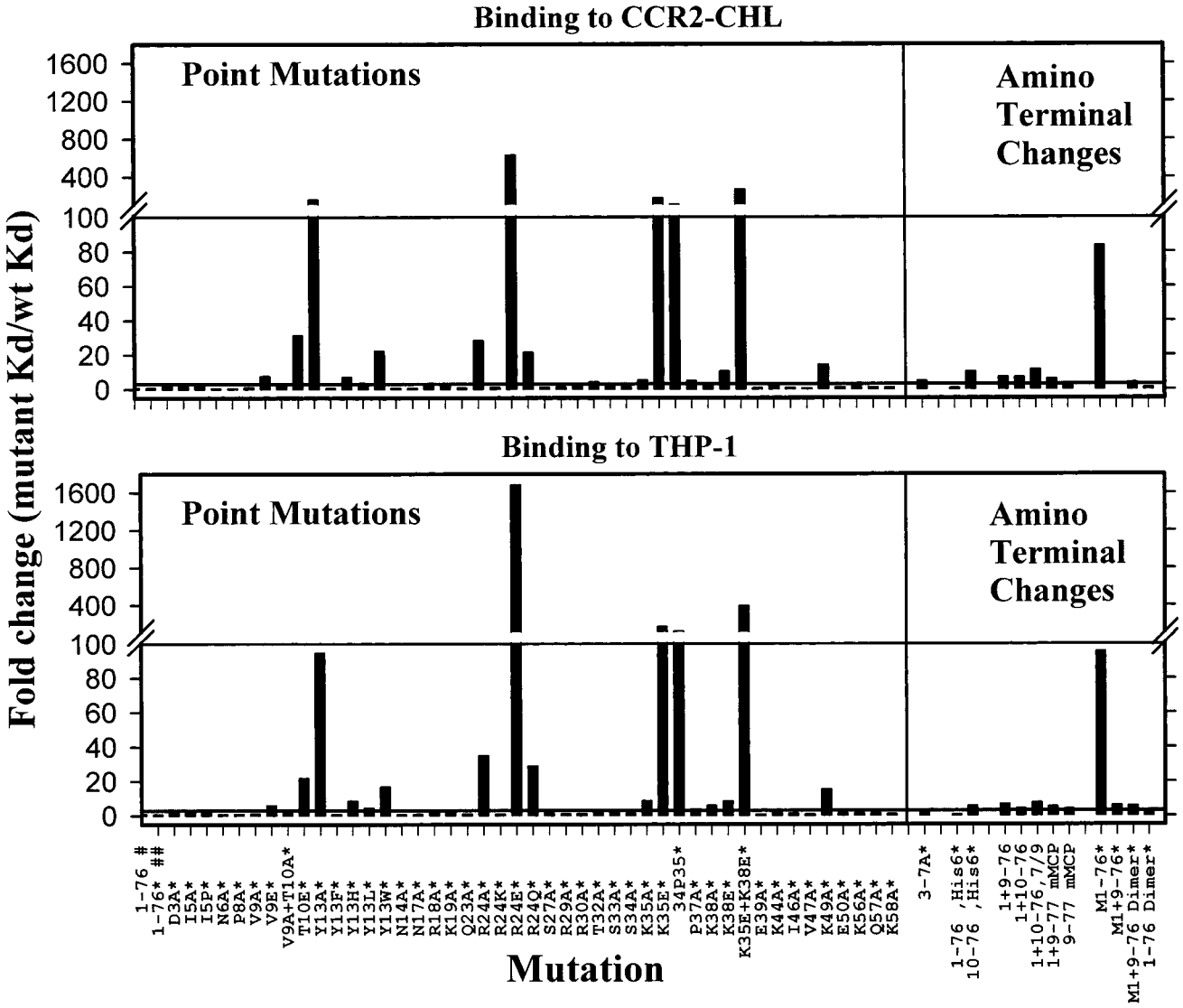

FIGURE 3: Summary of the binding affinity of various mutants to CCR2 on THP-1 cells and CCR2-CHL cells. The number plotted for each mutant is (the mutant K_d)/(the WT K_d). Each data point is the mean of at least duplicate and up to 441 replicate determinations. The relative standard deviation of the mean K_d averages 40 ± 21% for THP-1 cells and 38 ± 21% for CCR2-CHL cells. The mutant nomenclature is as follows. Unless otherwise indicated, all sequences are human. 1−76 represents full-length wild-type human MCP-1. A * represents a mutant in the M64I background. A # indicates wild-type MCP-1 from R&D Systems, while a ## indicates wild-type MCP-1 produced as described in Materials and Methods. Point mutations are denoted by noting the parent residue and its position followed by the single-letter code for the residue to which the parent was changed. Deletions are indicated by inclusion of the residues present in the product protein; thus, [1+9−76] indicates MCP-1 with residues 2−8 deleted. The mutant [1+10−76,7/9] indicates hMCP-1 with residues 2−9 deleted and seven of nine lysines changed to arginine or methionine (K75 and K69 were not mutated). In other words, [1+10−76,7/9] is [1+10−76,-K19M/K35R/K38R/K44R/K49R/K56R/K58R]hMCP-1. Mutants with His6 appended have six histidines added to the C-terminus of the full-length protein. Mutants preceded by an M retained the initiating methionine at the N-terminus. Dimer forms were made by the addition of a cysteine (Cys77) to the C-terminus which was then oxidized to form a disulfide bridge between Cys77 of two correctly folded monomers.

affinity (Figures 3 and 5a). Similarly, mutation of S33A in the 30's loop caused a 2−3-fold loss in affinity. All other mutations of surface-exposed residues showed insignificant changes in affinity (Figure 3).

The N-Terminal Residues Contribute Little to Binding Affinity, and Their Exact Chemical Nature Is Also Unimportant. Previous studies have shown that the N-terminus of MCP-1 is critical for receptor activation. These data were generated by sequentially truncating residues from the amino terminus of MCP-1 and assaying for binding and receptor activation. One of the most interesting analogues, [1+9−76]hMCP-1, exhibits high-affinity binding (level of binding reduced by 6−7-fold relative to that of WT in our hands; Figure 3) but as reported elsewhere (*32*, *36*), and reproduced by us (*41*), fails to induce chemotaxis and thus acts as a receptor antagonist. On the other hand, extension of the N-terminus by one residue, a Met which was not processed during bacterial expression, reduced the affinity by nearly 2 orders of magnitude (Figure 3). To further probe the role of specific residues in the N-terminus, we introduced a number of alanine substitutions. Previously, we showed that a P8A mutant was identical to WT* in binding affinity and biological activity (*41*). Individual point mutations of D3, I5, and N6 to Ala (residues 4 and 7 are Ala in the WT protein) reduced the level of binding by only a factor of 1.7−2.8, while the triple mutant D3A/I5A/N6A was only slightly worse (2.4−4.8-fold lower than that of WT). Even a highly nonconservative I5P mutation had little effect (1.8−2.8-fold);

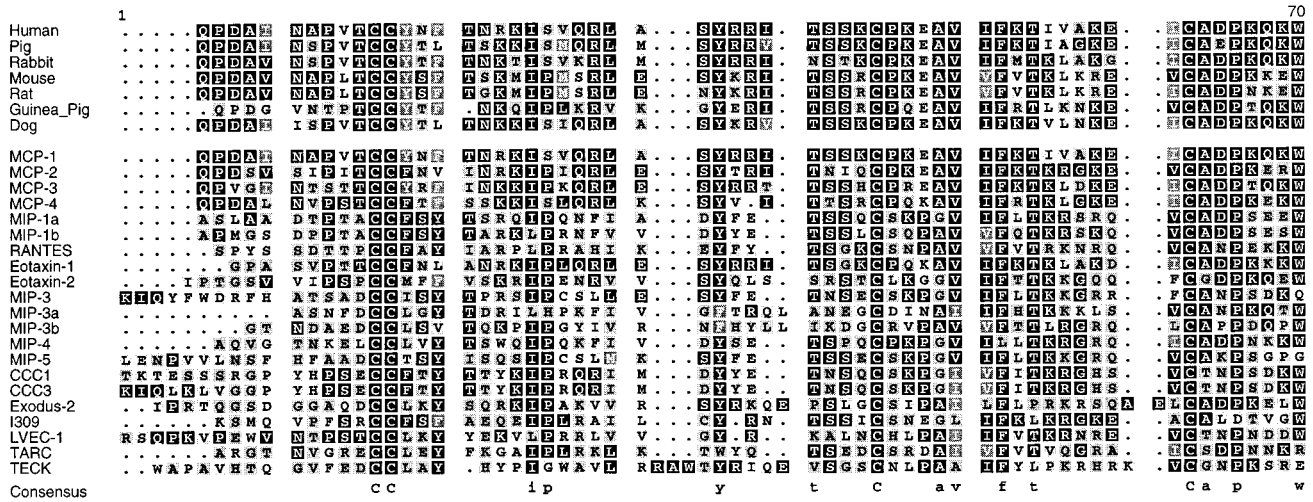

FIGURE 4: Sequence alignment of MCP-1 from various species and with other CC chemokines. Sequences are shown only up to residue 70.

preparation of this mutant was motivated by the fact that in the crystal structure of MCP-1 (*50*), residues 2−6 are involved in a single turn of 3^{10}-helix and insertion of Pro would be expected to disrupt the helix. Thus, it appears that the N-terminus accounts for very little of the 35 pM binding affinity of the whole protein. Moreover, the chemical nature of the residues is not critical, nor is the presence of helical secondary structure.

Small Constrained Peptides Have Micromolar Affinities and Reflect Some of the Important Structural Features of the Protein. Some of the important interactions observed in the intact protein can be recapitulated in the context of small peptides as summarized in Table 1. Although the N-terminal residues are required for signaling, as noted above, they contribute little to binding affinity. Consequently, it is not surprising that peptides corresponding to the first 10 (peptide 1) or 16 (peptide 2) amino acids are weak binders with K_d values of >100 μM. However, a linear peptide (peptide 3) spanning residues Y13−K35 (Figure 5a, the region highlighted in yellow) had an affinity of 48 μM, while truncation from either end of this peptide (peptides 4−6) caused a loss in affinity. Constraining peptide 3 with a single disulfide encompassing R24 (peptides 7 and 8) increased the affinity to 4.8−7.8 μM, probably by forcing the peptide chain to reverse direction as in the complete protein. A similar increase in affinity was achieved by restraining the ends of the peptide with a disulfide that approximates the C11−C36 disulfide in MCP-1 (peptide 10, Figure 5a). Introduction of both types of disulfides improved the affinity even further; the K_d values for peptide 11 and 12 were 2.1 and 2.0 μM, respectively. However, mutation of R18 and R24 to Ala in two peptides related to peptide 14 (18 and 19) caused a loss of affinity, consistent with the protein mutational studies. Surprisingly, smaller constrained peptides were also micromolar binders, the best being peptide 17 which spans residues N17−R30 and contains an internal disulfide surrounding R24 (K_d = 8.2 μM). These data support the importance of the first disulfide bridge, the region between residues 13 and 30, and specifically residues R24 and R18, in receptor binding.

NMR Spectra of MCP-1 Mutants Indicate That They Are Properly Folded. To rule out the possibility that the mutations

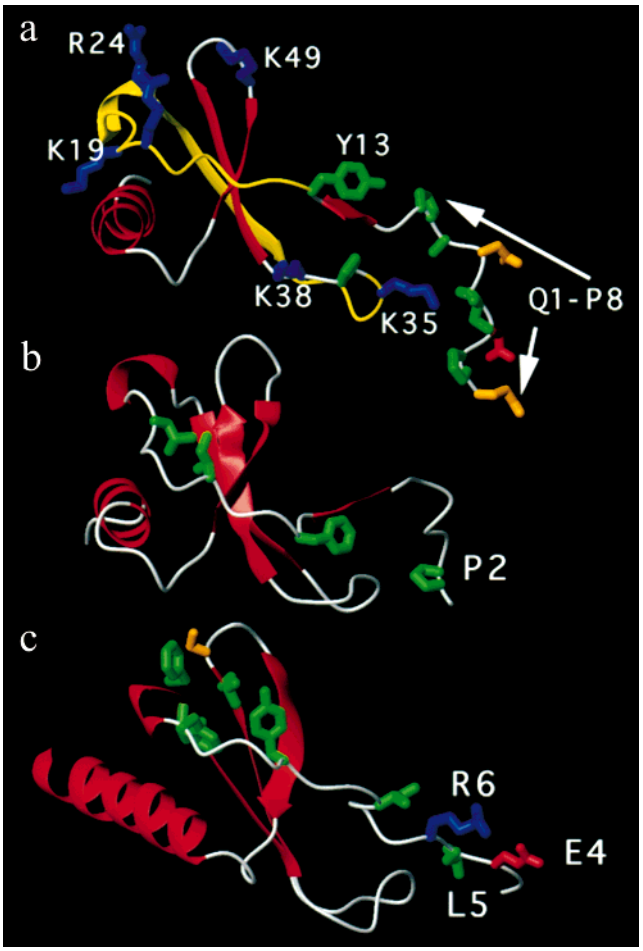

FIGURE 5: Molmol diagrams showing the locations of side chains which have the largest impact on binding. (a) MCP-1 binding to CCR2. The region corresponding to residues 13−35 (peptide 3 from Table 1) is highlighted in yellow. For comparison, (b) the receptor binding sites of RANTES for CCR5 (CCR3 and CCR1 epitopes have also been reported but are not shown here) (*63*) and (c) the receptor binding site of IL8 for CXCR1 (*62*, *68*, *73*, *74*). Side chains are colored blue, red, green, and orange for basic, acidic, hydrophobic, and other polar, respectively. The Molscript diagrams were generated using monomeric subunits derived from the NMR structures of MCP-1, RANTES, and IL8 (PDB file names 1DOM, 1RTO, and 1IL8).

Table 1: Summary of Binding Data for Peptide Fragments of MCP-1[a]

[1-76]hMCP-1		**35 pM**
1	QPDAINAPVT-nh2	>100uM
2	QPDAINAPVTSSYNFT-nh2	>100uM
3	Ac**YNFTNRKISVQRLASYRRITSSK**-nh2	**48** uM
4	AcYNFTNRKISVQR-nh2	>100uM
5	AcNRKISVQRLASYRR-nh2	>100uM
6	AcSVQRLASYRRITSSK-nh2	>100uM
7	Ac**YNFTNRKISCQRCASYRRITSSK**-nh2	**4.8uM**
8	Ac**YNFTNRKISCQRLASCRRITSSK**-nh2	**7.8uM**
9	AcYNF**K**NRK**E**SVQRLASYRRITSSK-nh2	**49 uM**
10	Ac**YCFTNRKISVQRLASYRRITCSK**-nh2	**4.7uM**
11	Ac**YCFTNRKISCQRCASYRRITCSK**-NH2	**2.1uM**
12	Ac**YCFTNRKISCQRLASCRRITCSK**-NH2	**2.0uM**
13	AcNRKIS**C**QR**C**ASYRRITSSK-nh2	**7.7uM**
14	AcYNFTNRKIS**C**QR**C**ASYRR-nh2	**10.8uM**
15	AcNRK**C**SVQR**C**ASYRR-nh2	**23.0uM**
16	AcNRKIS**C**QRLAS**C**RR-nh2	**17.9uM**
17	AcNRK**C**SVQRLAS**C**RR-nh2	**8.2uM**
18	AcYNFTN**A**KIS**C**QR**C**ASYRR-nh2	**20.6uM**
19	AcYNFTNRKIS**C**Q**AC**ASYRR-nh2	**72.2uM**

[a] The level of binding was measured on CCR2-CHL cells. The reported K_d values are the average of triplicate measurements. In the singly cyclic peptides, the underlined residues are disulfide bonded together except in peptide 9 which is linked by an amide bond. Brackets show the bonding pattern for all doubly cyclic peptides. The secondary structure of MCP-1 as derived from NMR and crystallographic studies is shown under the wild-type sequence with the following designations: s, β-sheet; ht, helical turn; and h, α-helix.

cause major structural perturbations, we recorded one-dimensional ^{1}H and two-dimensional ^{1}H$-^{15}$N HSQC spectra of WT* and mutants that had the largest impact on binding (R24A, K49A, K35A, 34P35, Y13A, [1+9−76]hMCP-1, and T10E). From these experiments, line widths, spectral dispersion, the number of cross-peaks, and particularly differences in chemical shifts can be used to assess the degree of structural change. In all cases, the spectra were well-dispersed, indicating that the mutations do not cause misfolding of the protein. The one-dimensional ^{1}H spectra of several variants (R24A, K49A, K35A, and T10E) exhibited two upfield-shifted resonances with chemical shifts identical to those observed in WT*, which were previously assigned to γ-methyl protons of V60 and V41 (*49*). These residues are shifted because of their close proximity to F43 in the core of the protein. Since the extent of the shift is very sensitive to the distance and orientation from the aromatic ring, preservation of the WT chemical shifts suggests that the core structures of these mutants are very similar to WT*.

For Y13A, [1+9−76]hMCP-1, P8A, and 34P35, the γ_1-methyl protons of V60 were shifted downfield by 0.05 ppm relative to those of WT*, indicating a small perturbation of core structure. Interestingly, this shift correlates with the aggregation state of the protein; Y13A, [1+9−76]hMCP-1, and P8A are all monomeric at high concentrations (*41*) in contrast to WT and other mutants which form dimers. We previously demonstrated that P8A has wild-type binding affinity and activity, indicating that MCP-1 binds CCR2 as a monomer (*41*). This suggests that the minor change in chemical shift does not reflect a structural perturbation that affects binding. On the basis of the similar chemical shift for 34P35, we predicted and subsequently confirmed that it is also monomeric (data not shown). Thus, it appears that the conformation of the 30's loop can be transmitted to the dimerization interface by virtue of the disulfide bond between C11 (in the dimer interface) and Cys36 in the 30's loop. 34P35 also has a 0.31 ppm upfield shift of the V41 γ_1-methyl proton not seen in any of the other mutants, indicating additional structural change in the protein core. However, this is not surprising given that it is a nonconservative insertional mutation.

The HSQC spectra were also well-dispersed and corroborate conclusions from the one-dimensional spectra. For analysis of the HSQC data, mutant proteins were divided into two groups according to their oligomeric state. Spectra of dimers were compared to the spectrum of the WT* protein,

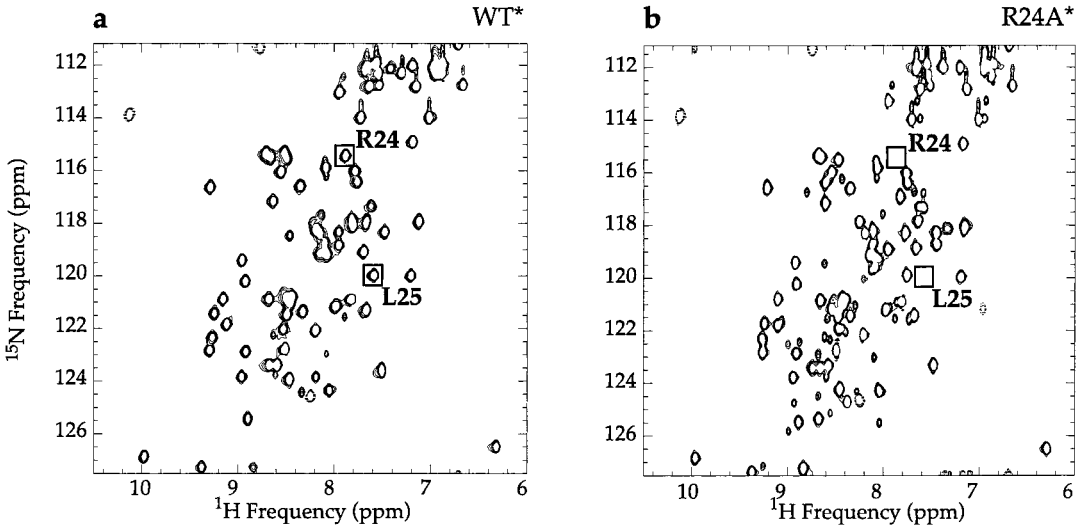

FIGURE 6: Representative subspectra from $^{1}H-^{15}N$ HSQCs of (a) WT* and (b) R24A. The similarity in the patterns of cross-peaks reflects the structural integrity of the mutants.

Table 2: Summary of Chemical Shift Changes in the HSQC Spectra of Several Mutants[a]

mutant	no change[b]	shifted[b]	not found
		Dimeric Variants	
T10E	36 resonances	R29, S33, I42, F43, K44	T10, C11, R30
R24A	42 resonances	L25	R24
K35A	36 resonances	V9, T10, C11, N14, F15, S33, K38	C36
K49A	41 resonances	T45, V47	K49
		Monomeric Variants	
mutant	no change[c]	shifted[c]	not found
[1+9−76]	42 resonances	T45, I46, K49, I51, W59	A4, I5
Y13A	39 resonances	T32, S33, E39, T45, I46, I51, W59	Y13, N14, F15, K35
34P35	33 resonances	F15, I31, S33, I42, F43, T45, I46, I51, C52, A53	Y13, N14, R30, T32, K35, E39

[a] For dimeric variants, the data indicate that the structures are nearly identical to WT* as chemical shift changes are localized to residues in the immediate vicinity of the site of mutation. For the monomeric variants, chemical shift changes relative to WT* are more extensive because of the loss of contacts at the dimer interface. Nevertheless, all monomeric mutant spectra resemble P8A, a variant which has WT binding affinity and activity, indicating these proteins are also properly folded. [b] Compared to WT*, 44 resonances are suitable for unambiguous comparison. [c] Compared to P8A*, 50 resonances are suitable for unambiguous comparison.

while spectra of monomeric variants were compared to the spectrum of P8A. Of the dimers, we have complete resonance assignments only for the WT protein (*49*). Nevertheless, it was possible to transfer assignments of 44 residues from the WT spectrum to that of WT* and the other dimeric mutants. These are dispersed throughout the protein and serve as probes for structural perturbations in local and remote regions of the mutations. Figure 6 shows representative subspectra of WT and R24A to illustrate the similarity in the patterns of chemical shifts. For R24A, K49A, T10E, and K35A, the largest chemical shift changes are largely localized to the region of the mutation (Table 2). For example, in the HSQC subspectra of R24A (Figure 6b), the only difference from WT* is a slight shift of L25. Elsewhere in the spectra, R24 is missing and I20 is slightly shifted. Because of the apparent coupling between the dimerization interface and the 30's loop described above, the T10E mutation impacts residues in the 30's loop and mutations in the 30's loop affect residues in the dimerization interface. However, the consistency of chemical shifts throughout the rest of the protein suggests that all of these mutants retain the WT structure with only small local perturbations.

As for the one-dimensional spectra, the mutants that exhibit significant differences in the HSQC spectra relative to that of WT* are those that are monomeric. For these mutants (Y13A, 34P35, P8A, and [1+9−76]hMCP-1), significant changes are expected due to the loss of extensive contacts at the dimerization interface (*41*). However, all of the spectra are very similar to the spectrum of P8A (Table 2). Backbone (H_N, ^{15}N, Cα, and Cβ) assignments have been made for P8A (L. Mizoue and T. Handel, manuscript in preparation), 50 of which could be transferred to the other mutants as probes of structure. Most probes were unshifted relative to P8A (Table 2). This indicates that apart from dimer formation, the mutations do not perturb structure to any significant extent, and the effects on binding can be safely attributed to the loss of direct contacts with the receptor. The exception is 34P35 which is well-folded but may have some conformational differences that compromise the orientation of key residues, such as Y13 or the N-terminus, with the receptor, accounting for its large reduction in binding affinity.

Amino-Terminal Mutations of the MCP-1 Receptor, CCR2, Suggest Important Features of the Receptor−Ligand Interaction. Because most of the residues that contribute significantly to binding affinity are basic, we examined the receptor for acidic residues which might be involved in electrostatic interactions with the ligand. There are 13 negatively charged residues in the extracellular domains and transmembrane helices of CCR2. Five of these are located in the amino terminus in a stretch of 14 amino acids (residues 15−28). This region features two clusters of negatively charged residues separated by a hydrophobic region (sequence being ESGEEVTTFFDYDY) that complements the two basic patches separated by a hydrophobic groove on MCP-1. Since the receptor N-terminus has been shown to be an important ligand binding determinant by mutagenesis for CXCR1 and

Table 3: Summary of Acidic to Ala Mutations in CCR2

mutant	K_d (nM)[a] mean ± SD	K_d (nM)[a] *N*	fluorescence intensity[b] mean ± SD	fluorescence intensity[b] *N*	no. of receptors per cell mean ± SD	no. of receptors per cell *N*	K_d ratio (mutant/WT)
WT	0.06 ± 0.01	8	302 ± 147	10	21000 ± 8000	7	1.0
D36A	0.04 ± 0.01	3	74 ± 20	3	6000 ± 1000	3	0.7
D25A/D27A	>3	4	15[c] ± 1	3	UTM[d]	4	>50
E15A/E18A/E19A	0.12 ± 0.05	3	240 ± 55	3	11000 ± 2000	3	2.0

[a] K_d values were determined via saturation binding using [^{125}I]MCP-1. [b] Shown is the fold increase in fluorescence intensity of the transfected cell line over that of the untransfected L1.2 control line. [c] Two stable populations were present. The mean fold increase of the more brightly fluorescent population is shown. The two populations were present after two rounds of single cell cloning. [d] UTM means unable to measure, since saturation was not achieved at 3 nM [^{125}I]MCP-1.

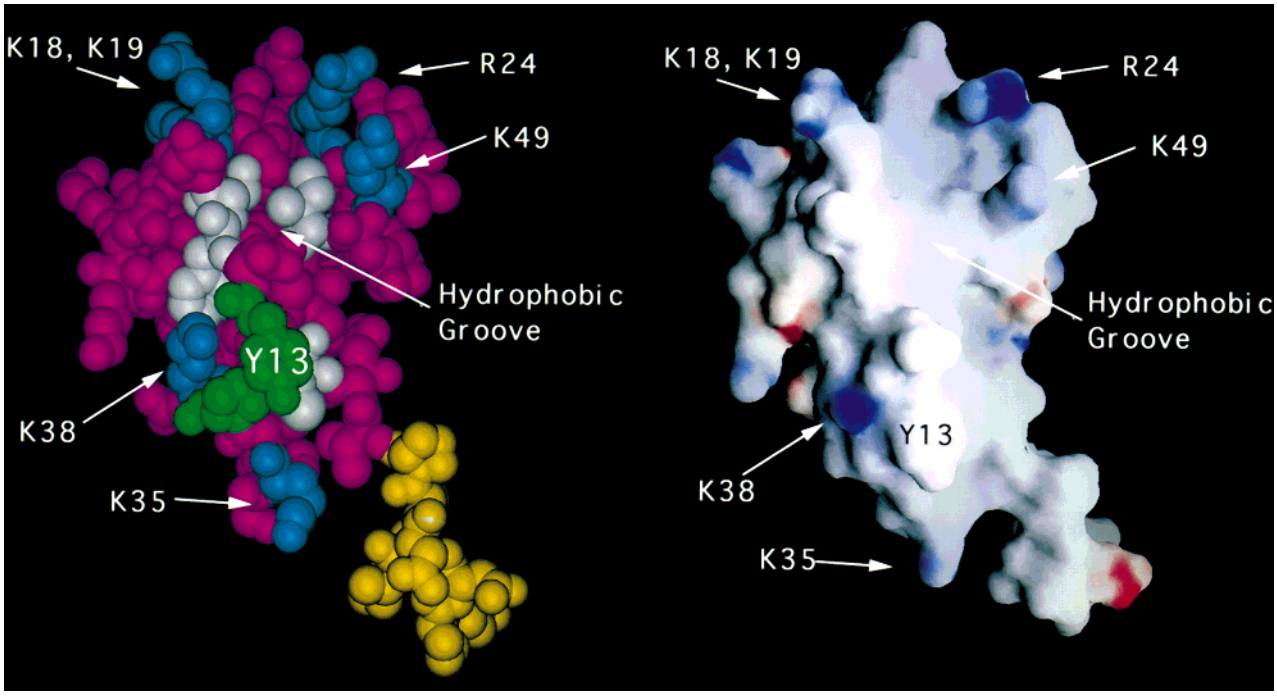

FIGURE 7: Two views of MCP-1 highlighting the residues which interact with CCR2. (Left) CPK model with residues which do not affect binding (or were not mutated) shown in pink. The eight N-terminal residues which together contribute less than a factor of 10 to binding affinity, but are important for signaling, are shown in yellow. Basic residues (K18, K19, R25, K35, K38, and K49) are shown in blue; hydrophobic residues, Y13 and P37, are shown in green. C11, F15, T16, and I51 are shown in gray; these residues were identified by NMR (L. Mizoue and T. Handel, manuscript in preparation) and cluster in the hydrophobic pocket bounded by the basic residues and Y13 (see the text). (Right) Surface electrostatic model illustrating the hydrophobic groove which extends between the two patches of basic residues. Electrostatic potentials were calculated within GRASP (*75*) using the Poisson−Boltzmann equation and are indicated by blue for positive and red for negative.

-2 (*56*, *57*), CCR2 (*1*), and DARC (*58*), and by NMR for CXCR1 (*59*, *60*), CX_3CR1 (*61*), and CCR2 (L. Mizoue and T. Handel, manuscript in preparation), we mutated the charged N-terminal residues in CCR2 to Ala, and examined their impact on binding.

Table 3 summarizes the binding affinities of the mutant receptors. A triple mutant containing E15, E18, and E19 is clearly unimportant for binding as the affinity for MCP-1 is only 2-fold higher than that of the wild-type receptor. The affinity of the single-point mutation of D36A is 0.7-fold lower than that of the wild-type receptor, again an insignificant change. In contrast, the double mutant D25A/D27A has no measurable affinity up to 3 nM MCP-1. This change of at least 50-fold in binding affinity is highly significant and demonstrates the importance of these residues in ligand binding.

DISCUSSION

A number of studies have identified residues in chemokines that are important for receptor interaction, but the molecular details of how chemokines bind and activate their receptors remain incomplete. Here we have undertaken a comprehensive mutagenesis study of MCP-1 to determine which residues are important for binding. Mutants which had a significant effect on affinity were ^{15}N-labeled and characterized by one-dimensional ^{1}H and two-dimensional ^{1}H−^{15}N HSQC spectra to ensure that the mutations did not cause structural perturbations. In all cases, chemical shift changes were localized to the site of mutation. Therefore, we can be certain that the indicated residues make direct contacts with CCR2.

MCP-1 Binding Surface As Suggested by Mutagenesis, Peptide Studies, and NMR Data. Figure 7 shows CPK models of MCP-1 highlighting the residues which showed the largest effects on binding. Apart from the N-terminal region, the data define two patches of primarily basic residues which are separated by approximately 35 Å. Together with the N-terminus, these mutations account for approximately 50% of the binding affinity for the receptor. Therefore, the affinity which is not accounted for must come from interactions with

backbone atoms, the structurally important cysteine residues, or hydrophobic interactions with apolar residues that were not mutated because such mutations would probably alter protein structure. One candidate region is a shallow hydrophobic groove that spans the two basic clusters (Figure 7). We have evidence from NMR studies (L. Mizoue and T. Handel, manuscript in preparation) that several residues in this groove, particularly C11, F15, T16, and I51, make contacts with the N-terminus of the receptor, which was previously identified as an important binding determinant in CCR2 (*1*). Additional residues ranging from the dimer interface at one end of the molecule to R18 and K19 at the other end are also perturbed in the NMR studies, suggesting that the receptor N-terminus spans the surface of MCP-1 in an extended fashion. This hypothesis is supported by the recently determined structure of a complex between the receptor N-terminus of CXCR1 and IL-8 (*60*).

Comparison to Other Chemokines. An important question is how chemokines discriminate between different receptors because all structurally characterized chemokines have very similar tertiary structures. Thus, specificity must be due to a combination of subtle conformational and sequence differences. With such an extensive mutational analysis, we are now in a position to address the issue of specificity by comparing the CCR2 binding site of MCP-1 to the binding surface of other chemokines. Figure 5 shows ribbon diagrams of MCP-1, RANTES, and IL-8, with residues that are important for binding highlighted according to charge and hydrophobicity. From a cursory inspection, one can see that there are some similarities but also significant differences in the chemical nature and distribution of residues that constitute the binding sites.

In all three cases, N-terminal residues are important for binding and particularly receptor signaling. For MCP-1, we have shown that the amino terminus contributes little to affinity and that the exact sequence is not important; mutation of D3, N6, and I7 altered the level of binding by less than a factor of 5, and deletion of eight or nine residues at the N-terminus reduced the level of binding by <7-fold. However, the deletion has been shown previously to completely inhibit chemotaxis (*32*, *37*). Nevertheless, the triple mutant D3A/N6A/I7A retains the ability to drive chemotaxis (K. Jarnagin et al., manuscript submitted for publication). Taken together, these data suggest that the presence of a polypeptide chain of the correct length is the most critical requirement. By contrast, the precise ELR motif of IL-8 (E4, L5, and R6; Figure 5c) has been known to be crucial for the interaction with CXCR1 and -2. Ala mutations of any one of these residues causes a 100−1000-fold loss in affinity, and the triple mutant is completely inactive in calcium assays (*62*). Likewise, RANTES binding to CCR5 (Figure 5b) is dependent on the presence of P2; mutation to Ala results in a 5000-fold loss of affinity (*63*) and virtually no calcium response. Thus, the chemical nature of these residues and how much they contribute to affinity are entirely different among these three chemokines.

One similarity between RANTES and MCP-1 is that extension of the N-terminus by a methionine leads to a reduction in affinity [95-fold for MCP-1 (Figure 3) and 10−15-fold for RANTES]. In the case of RANTES, the resulting protein acts as a receptor antagonist (*64*). Elsewhere, we show that in MCP-1, the Met also causes a significant loss of bioactivity (K. Jarnagin et al., manuscript submitted for publication) which is consistent with previous reports that extension with Ala completely impairs chemotaxis (*39*). These effects may occur by a steric mechanism whereby the additional Met prevents the critical N-terminal residues from making productive contacts with the receptor. Following the observation that one can modulate signaling without significantly interfering with binding, Simmons and co-workers made a chemically derivitized form of RANTES (aminooxypentane−RANTES) which retains nanomolar affinity but is a potent receptor antagonist of CCR5 (*65*). The similarity in the consequences of Met extensions of MCP-1 and RANTES suggests that aminooxypentane−MCP-1 might also function as a receptor antagonist of CCR2.

For each of these proteins, particularly MCP-1, much of the binding energy comes from the core domain (everything excluding the N-terminus). Of the surface-exposed residues in MCP-1, Y13 contributes the most to binding affinity. The corresponding residues in RANTES and IL-8 are F12 and I10, respectively; mutation of these to alanine caused 5000- and 100-fold reductions in affinity for CCR3/CCR5 (RANTES receptors) and CXCR1 (IL-8 receptor), respectively. Thus, residues immediately following the first two cysteines may be a common recognition element in chemokines. Like Y13 in MCP-1, F12 is buried in the dimer interface of RANTES, and it was postulated that the dimer could be the active species for binding to the receptor (*63*). However, we feel that this is unlikely because we previously demonstrated that a P8A mutant of MCP-1 is as active as WT, even though it does not dimerize (*41*). Therefore, these residues probably directly contact their receptors in the context of the monomer structures. This further implies that to bind and activate their receptors, subunit dissociation must be required for MCP-1 and RANTES. This contrasts with IL-8 which does not require subunit dissociation for binding (*66*), presumably because I10 is not involved in formation of the IL-8 dimer.

Additional hydrophobic residues in the so-called "N-loop" (residues between the second cysteine and the 3^{10}-helix; i.e., residues 13−20 in MCP-1) have been shown to be important for IL-8 receptor binding and for determining the specificity of MGSA for IL-8 receptors CXCR1 and -2 (*67*). The key residues in IL-8 include Y13, F17, F21, and I22 (*67*, *68*). These cluster to form a large hydrophobic pocket well separated from the ELR motif (Figure 5c). In RANTES, two hydrophobic residues (I15 and L19) also contribute significantly to binding CCR5; mutation to Ala caused a >5000-fold reduction in affinity (*63*). For MCP-1, mutation of many of the N-loop residues had little or no effect. Small changes were observed for two basic residues, R18 (demonstrated primarily by peptide 18, Table 1) and K19 (Figure 3). Other buried hydrophobic residues in the MCP-1 N-loop were not mutated because they were expected to affect folding of the protein. However, as previously mentioned, we have NMR evidence (L. Mizoue and T. Handel, manuscript in preparation) that F15 and T16 (and I51) interact with the N-terminus of the receptor (not shown in Figure 5a). Interestingly, T16 is highly conserved across different MCP-1 sequences and is the equivalent of I15 in RANTES. We have also demonstrated a qualitatively similar interaction of the N-terminus of CX_3CR1 with this region of fractalkine by NMR (*61*). Likewise an N-terminal peptide of CXCR1 was shown to bind to the N-loop of IL-8 (*59*, *60*). Thus, the N-loop

may be a common recognition element involved in chemokine−receptor interactions, but the nature and distribution of the residues may impart specificity.

Following the N-loop and immediately adjacent to the 3^{10}-helix, R24, a completely conserved residue in MCP-1 sequences, had the second largest impact on binding to CCR2 (Figure 5a). The corresponding residue in IL-8 is I22 (*68*) which altered binding to the IL-8 receptor by approximately the same magnitude (Figure 5c). Thus, this may also be a binding and specificity-determining position in many chemokines. Basic residues in MCP-1 (K35, K38, and K49) are also important for binding and cluster together in two patches that are separated by a hydrophobic groove (Figures 5a and 7). Although extensive mutagenesis has been carried out on IL-8, analogous basic motifs have not been reported. Overall, it appears that the receptor binding site on IL-8 (Figure 5c) is significantly more hydrophobic than that on MCP-1 (Figure 5a).

Interaction with the Receptor. In light of the basic and hydrophobic binding surface illustrated in Figure 7, the work by Monteclaro and co-workers which demonstrates the importance of the CCR2 N-terminus (*1*), NMR data which show that the CCR2 N-terminus interacts with a large surface area of MCP-1 (T. Handel and L. Mizoue, manuscript in preparation), and the complementary acidic and hydrophobic nature of the CCR2 N-terminus, we mutated acidic residues in the receptor to further test ideas about the ligand−receptor interaction. In particular, the sequence 15-ESGEEVTTFFDY-DY-28 contains two clusters of acidic residues separated by several hydrophobic residues. Simple molecular docking of this sequence in an extended conformation onto MCP-1 suggested that the peptide could span the 35 Å between the two basic patches, allowing interaction of the basic residues of the ligand and the acidic residues of the receptor. The mutational analysis demonstrated the importance of D25 and D27 for the receptor−ligand interaction. However, E15, E18, E19, and D36 do not appear to play a significant role.

Interestingly, D25 and D27 are part of a DYDY motif which is a signature sequence for tyrosine sulfation. This is a post-translational modification which occurs at the N-terminus of CCR5 and is important for both chemokine binding and HIV infection (*69*). Tyrosine sulfation could serve as a general mechanism for achieving specificity in chemokine−receptor recognition. Whether one or both tyrosines in CCR2 are sulfated and whether mutation of D25 or D27 affects binding directly, or indirectly by affecting sulfation, is under investigation. US28, a viral chemokine that binds MCP-1, also has a DYD sequence, suggesting that at least the first tyrosine in CCR2 may be important:

```
CCR2(19-32):  EVTTFFDYDYGA PC
US28(9-23):   ELTTEFDYDDEATPC
```

In any event, it is likely that the acidic DYDY sequence interacts with one of the basic patches of the ligand. We suspect that the interaction is with R24 and K49, and to a lesser extent with R18 and K19, because of their relative orientations and contributions to binding affinity as determined from mutagenesis and peptide studies. Recall that an R24E mutation also significantly decreased the level of binding, implicating R24 in an interaction with a negatively charged residue.

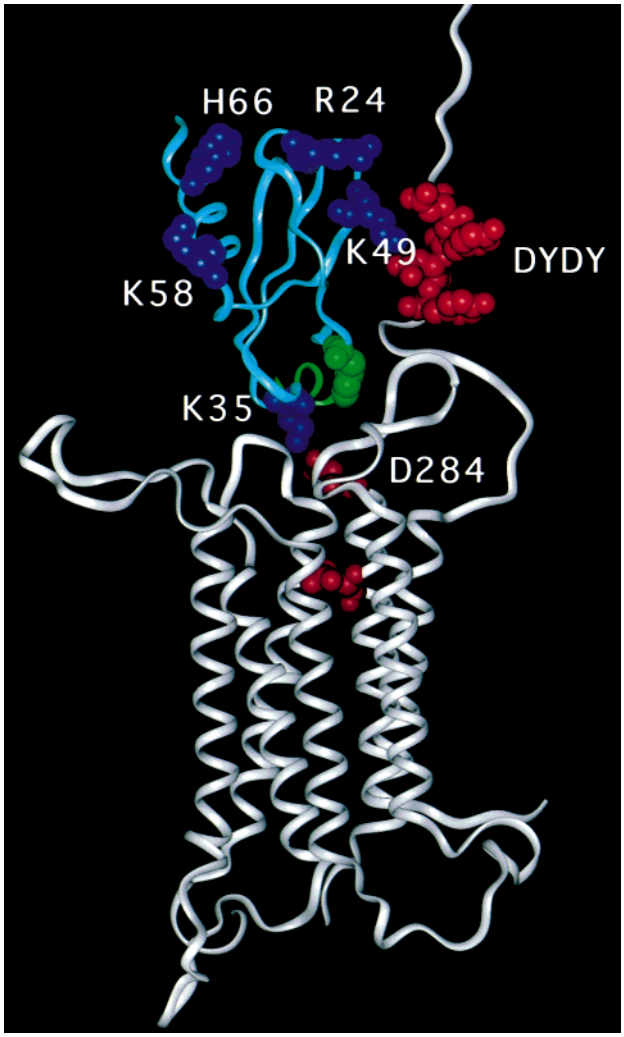

FIGURE 8: Low-resolution model for the interaction of MCP-1 with CCR2. A monomeric subunit of MCP-1 from the crystal structure is shown in light blue. A model of CCR2 is shown in gray. Side chains of the DYDY sequence in the receptor N-terminus and D284 and E291 in TM-7 are shown in red. The side chains of R24 and K49 of MCP-1 (dark blue) are docked in close proximity to the DYDY sequence of the receptor. K35 (dark blue) of MCP-1 is shown in close proximity to D284 of the receptor. The side chains of K58 and H66 (dark blue) are shown pointing away from the receptor, allowing for possible interaction with glycosaminoglycans on an endothelial cell surface. The key signaling residues (Y13 and the N-terminus) are shown in green.

We also introduced mutations of two other negatively charged residues into the receptor, D284A and E291A at the top of TM-7. These mutations affected MCP-1 binding by factors of 4.7- and 8.5-fold, respectively, and also impaired small molecule antagonist binding (T. Mirzadegan et al., manuscript in preparation). While we cannot rule out the possibility that the mutations cause structural perturbations of the receptor and indirectly affect binding, it is possible that one of these acidic residues interacts with K35, at the opposite end of the hydrophobic groove from R24 and K49.

At this point, we can only construct a very crude model of the interactions we have observed, but such a model can be used to generate hypotheses and guide further mutagenesis and structural studies. In Figure 8, we illustrate the MCP-1−receptor complex using a monomer of MCP-1, since previous studies demonstrated that a monomeric mutant had

wild-type binding affinity and activity (*70*). Included in the model is the interaction of the receptor N-terminal DYDY motif and the basic patch, including R24 and K49 on MCP-1, an interaction of which we are fairly confident. Our NMR data suggested additional interactions between residues from the receptor N-terminus and the hydrophobic groove of MCP-1. The most likely candidates are residues preceding (VTTFF) or following (GAPC) the DYDY motif, which we are testing. In the model, we have placed K35 of MCP-1 in close proximity to the charged residues of TM-7, although this remains to be proven. Whether the interaction of the crucial signaling residues (Y13 and the N-terminus of MCP-1) occurs within the helices or with the extracellular loops of the receptor, and where, also remains to be determined. Finally, two residues which have been identified as important for binding to glycosaminoglycans (GAGs) have been included (*71*).

In summary, these studies are beginning to illuminate some of the similar and distinguishing molecular features of chemokine−receptor recognition. On the ligand side, the hydrophobic groove formed by the N-loop appears to be a common binding determinant for CC, CXC, and CX_3C chemokines, while the N-terminus controls signaling. On the receptor side, the N-terminus appears to bind into the N-loop pocket of the ligand, and at least in the case of RANTES and MCP-1, DY motifs are utilized. Interestingly, the receptor N-terminus also seems to be important for the unrelated GPCR, C5A (*72*). Despite these common recognition elements, the chemical details of the receptor binding sites are very different as is the nature of residues required for receptor signaling (K. Jarnagin et al., manuscript submitted for publication). This bodes well for exploiting these differences in targeting specific receptors with antagonists in the treatment of inflammatory diseases.

SUPPORTING INFORMATION AVAILABLE

Table of the binding data, including replicate statistics. This material is available free of charge via the Internet at http://pubs.acs.org.

REFERENCES

1. Monteclaro, F. S., and Charo, I. F. (1996) *J. Biol. Chem. 271*, 19084−92.
2. Monteclaro, F. S., and Charo, I. F. (1997) *J. Biol. Chem. 272*, 23186−90.
3. Rollins, B. J. (1997) *Blood 90*, 909−28.
4. Proost, P., Wuyts, A., and van Damme, J. (1996) *Int. J. Clin. Lab. Res. 26*, 211−23.
5. Graves, D. T., and Jiang, Y. (1995) *Crit. Rev. Oral Biol. Med. 6*, 109−18.
6. Howard, O. M., Ben-Baruch, A., and Oppenheim, J. J. (1996) *Trends Biotechnol. 14*, 46−51.
7. Wells, T. N., Power, C. A., Lusti-Narasimhan, M., Hoogewerf, A. J., Cooke, R. M., Chung, C. W., Peitsch, M. C., and Proudfoot, A. E. (1996) *J. Leukocyte Biol. 59*, 53−60.
8. Bazan, J. F., Bacon, K. B., Hardiman, G., Wang, W., Soo, K., Rossi, D., Greaves, D. R., Zlotnik, A., and Schall, T. J. (1997) *Nature 385*, 640−4.
9. Kelner, G. S., Kennedy, J., Bacon, K. B., Kleyensteuber, S., Largaespada, D. A., Jenkins, N. A., Copeland, N. G., Bazan, J. F., Moore, K. W., Schall, T. J., et al. (1994) *Science 266*, 1395−9.
10. Pan, Y., Lloyd, C., Zhou, H., Dolich, S., Deeds, J., Gonzalo, J. A., Vath, J., Gosselin, M., Ma, J., Dussault, B., Woolf, E., Alperin, G., Culpepper, J., Gutierrez-Ramos, J. C., and Gearing, D. (1997) *Nature 387*, 611−7.
11. Grewal, I. S., Rutledge, B. J., Fiorillo, J. A., Gu, L., Gladue, R. P., Flavell, R. A., and Rollins, B. J. (1997) *J. Immunol. 159*, 401−8.
12. Nakamura, K., Williams, I. R., and Kupper, T. S. (1995) *J. Invest. Dermatol. 105*, 635−43.
13. Gunn, M. D., Nelken, N. A., Liao, X., and Williams, L. T. (1997) *J. Immunol. 158*, 376−83.
14. Fuentes, M. E., Durham, S. K., Swerdel, M. R., Lewin, A. C., Barton, D. S., Megill, J. R., Bravo, R., and Lira, S. A. (1995) *J. Immunol. 155*, 5769−76.
15. Rollins, B. J. (1996) *Mol. Med. Today 2*, 198−204.
16. Kunkel, S. L., Lukacs, N., Kasama, T., and Strieter, R. M. (1996) *J. Leukocyte Biol. 59*, 6−12.
17. Robinson, E., Keystone, E. C., Schall, T. J., Gillett, N., and Fish, E. N. (1995) *Clin. Exp. Immunol. 101*, 398−407.
18. Loetscher, P., Dewald, B., Baggiolini, M., and Seitz, M. (1994) *Cytokine 6*, 162−70.
19. Koch, A. E., Kunkel, S. L., Harlow, L. A., Johnson, B., Evanoff, H. L., Haines, G. K., Burdick, M. D., Pope, R. M., and Strieter, R. M. (1992) *J. Clin. Invest. 90*, 772−9.
20. Villiger, P. M., Terkeltaub, R., and Lotz, M. (1992) *J. Immunol. 149*, 722−7.
21. Hsieh, K. H., Chou, C. C., and Chiang, B. L. (1996) *J. Allergy Clin. Immunol. 98*, 580−7.
22. Kurashima, K., Mukaida, N., Fujimura, M., Schroder, J. M., Matsuda, T., and Matsushima, K. (1996) *J. Leukocyte Biol. 59*, 313−6.
23. Alam, R., York, J., Boyars, M., Stafford, S., Grant, J. A., Lee, J., Forsythe, P., Sim, T., and Ida, N. (1996) *Am. J. Respir. Crit. Care Med. 153*, 1398−404.
24. Sugiyama, Y., Kasahara, T., Mukaida, N., Matsushima, K., and Kitamura, S. (1995) *Eur. Respir. J. 8*, 1084−90.
25. Yla-Herttuala, S., Lipton, B. A., Rosenfeld, M. E., Sarkioja, T., Yoshimura, T., Leonard, E. J., Witztum, J. L., and Steinberg, D. (1991) *Proc. Natl. Acad. Sci. U.S.A. 88*, 5252−6.
26. Nelken, N. A., Coughlin, S. R., Gordon, D., and Wilcox, J. N. (1991) *J. Clin. Invest. 88*, 1121−7.
27. Flory, C. M., Jones, M. L., and Warren, J. S. (1993) *Lab. Invest. 69*, 396−404.
28. Lukacs, N. W., Strieter, R. M., Warmington, K., Lincoln, P., Chensue, S. W., and Kunkel, S. L. (1997) *J. Immunol. 158*, 4398−404.
29. Zisman, D. A., Kunkel, S. L., Strieter, R. M., Tsai, W. C., Bucknell, K., Wilkowski, J., and Standiford, T. J. (1997) *J. Clin. Invest. 99*, 2832−6.
30. Wenzel, U., Schneider, A., Valente, A. J., Abboud, H. E., Thaiss, F., Helmchen, U. M., and Stahl, R. A. (1997) *Kidney Int. 51*, 770−6.
31. Rand, M. L., Warren, J. S., Mansour, M. K., Newman, W., and Ringler, D. J. (1996) *Am. J. Pathol. 148*, 855−64.
32. Gong, J. H., Ratkay, L. G., Waterfield, J. D., and Clark-Lewis, I. (1997) *J. Exp. Med. 186*, 131−7.
33. Kuziel, W. A., Morgan, S. J., Dawson, T. C., Griffin, S., Smithies, O., Ley, K., and Maeda, N. (1997) *Proc. Natl. Acad. Sci. U.S.A. 94*, 12053−8.
34. Lu, B., Rutledge, B. J., Gu, L., Fiorillo, J., Lukacs, N. W., Kunkel, S. L., North, R., Gerard, C., and Rollins, B. J. (1998) *J. Exp. Med. 187*, 601−8.
35. Gu, L., Okada, Y., Clinton, S. K., Gerard, C., Sukhova, G. K., Libby, P., and Rollins, B. J. (1998) *Mol. Cell 2*, 275−81.
36. Zhang, Y., and Rollins, B. J. (1995) *Mol. Cell. Biol. 15*, 4851−5.
37. Zhang, Y. J., Rutledge, B. J., and Rollins, B. J. (1994) *J. Biol. Chem. 269*, 15918−24.
38. Beall, C. J., Mahajan, S., Kuhn, D. E., and Kolattukudy, P. E. (1996) *Biochem. J. 313*, 633−40.
39. Gong, J. H., and Clark-Lewis, I. (1995) *J. Exp. Med. 181*, 631−40.
40. Beall, C. J., Mahajan, S., and Kolattukudy, P. E. (1992) *J. Biol. Chem. 267*, 3455−9.

41. Paavola, C., Hemmerich, S., Grunberger, D., Polsky, I., Bloom, A., Freedman, R., Mulkins, M., Bhakta, S., McCarley, D., Wiesent, L., Wong, B., Jarnagin, K., and Handel, T. (1998) *J. Biol. Chem. 273*, 33157−65.
42. Wade, J. D., Fitzgerald, S. P., McDonald, M. R., McDougall, J. G., and Tregear, G. W. (1986) *Biopolymers 25*, S21−37.
43. King, D. S., Fields, C. G., and Fields, G. B. (1990) *Int. J. Pept. Protein Res. 36*, 255−66.
44. Otoka, A., Koide, T., Shide, A., and Fujii, N. (1991) *Tetrahedron Lett. 32*, 1223−6.
45. Jarnagin, K., Bhakta, S., Zuppan, P., Yee, C., Ho, T., Phan, T., Tahilramani, R., Pease, J. H., Miller, A., and Freedman, R. (1996) *J. Biol. Chem. 271*, 28277−86.
46. Grzesiek, S., and Bax, A. (1993) *J. Am. Chem. Soc. 115*, 12593−4.
47. Wishart, D. S., Bigam, C. G., Yao, J., Abildgaard, F., Dyson, H. J., Oldfield, E., Markley, J. L., and Sykes, B. D. (1995) *J. Biomol. NMR 6*, 135−40.
48. Sharp, K. A., Nicholls, A., Friedman, R., and Honig, B. (1991) *Biochemistry 30*, 9686−97.
49. Handel, T. M., and Domaille, P. J. (1996) *Biochemistry 35*, 6569−84.
50. Lubkowski, J., Bujacz, G., Boque, L., Domaille, P. J., Handel, T. M., and Wlodawer, A. (1997) *Nat. Struct. Biol. 4*, 64−9.
51. Skelton, N. J., Aspiras, F., Ogez, J., and Schall, T. J. (1995) *Biochemistry 34*, 5329−42.
52. Fairbrother, W. J., Reilly, D., Colby, T. J., Hesselgesser, J., and Horuk, R. (1994) *J. Mol. Biol. 242*, 252−70.
53. Lodi, P. J., Garrett, D. S., Kuszewski, J., Tsang, M. L., Weatherbee, J. A., Leonard, W. J., Gronenborn, A. M., and Clore, G. M. (1994) *Science 263*, 1762−7.
54. Clore, G. M., Appella, E., Yamada, M., Matsushima, K., and Gronenborn, A. M. (1990) *Biochemistry 29*, 1689−96.
55. Wells, J. A. (1990) *Biochemistry 29*, 8509−17.
56. LaRosa, G. J., Thomas, K. M., Kaufmann, M. E., Mark, R., White, M., Taylor, L., Gray, G., Witt, D., and Navarro, J. (1992) *J. Biol. Chem. 267*, 25402−6.
57. Gayle, R. B. d., Sleath, P. R., Srinivason, S., Birks, C. W., Weerawarna, K. S., Cerretti, D. P., Kozlosky, C. J., Nelson, N., Vanden Bos, T., and Beckmann, M. P. (1993) *J. Biol. Chem. 268*, 7283−9.
58. Lu, Z. H., Wang, Z. X., Horuk, R., Hesselgesser, J., Lou, Y. C., Hadley, T. J., and Peiper, S. C. (1995) *J. Biol. Chem. 270*, 26239−45.
59. Clubb, R. T., Omichinski, J. G., Clore, G. M., and Gronenborn, A. M. (1994) *FEBS Lett. 338*, 93−7.
60. Skelton, N., Quan, C., Reilly, D., and Lowman, H. (1999) *Struct. Folding Des. 7*, 157−68.
61. Mizoue, L. S., Bazan, J. F., Johnson, E. C., and Handel, T. M. (1999) *Biochemistry 38*, 1402−14.
62. Hebert, C. A., Vitangcol, R. V., and Baker, J. B. (1991) *J. Biol. Chem. 266*, 18989−94.
63. Pakianathan, D. R., Kuta, E. G., Artis, D. R., Skelton, N. J., and Hebert, C. A. (1997) *Biochemistry 36*, 9642−8.
64. Proudfoot, A. E., Power, C. A., Hoogewerf, A. J., Montjovent, M. O., Borlat, F., Offord, R. E., and Wells, T. N. (1996) *J. Biol. Chem. 271*, 2599−603.
65. Simmons, G., Clapham, P. R., Picard, L., Offord, R. E., Rosenkilde, M. M., Schwartz, T. W., Buser, R., Wells, T. N. C., and Proudfoot, A. E. (1997) *Science 276*, 276−9.
66. Leong, S. R., Lowman, H. B., Liu, J., Shire, S., Deforge, L. E., Gillece-Castro, B. L., McDowell, R., and Hebert, C. A. (1997) *Protein Sci. 6*, 609−17.
67. Lowman, H. B., Slagle, P. H., DeForge, L. E., Wirth, C. M., Gillece-Castro, B. L., Bourell, J. H., and Fairbrother, W. J. (1996) *J. Biol. Chem. 271*, 14344−52.
68. Williams, G., Borkakoti, N., Bottomley, G. A., Cowan, I., Fallowfield, A. G., Jones, P. S., Kirtland, S. J., Price, G. J., and Price, L. (1996) *J. Biol. Chem. 271*, 9579−86.
69. Farzan, M., Mirzabekov, T., Kolchinsky, P., Wyatt, R., Cayabyab, M., Gerard, N. P., Gerard, C., Sodroski, J., and Choe, H. (1999) *Cell 96*, 667−76.
70. Paavola, C., Hemmerich, S., Grunberger, D., Polsky, I., Bloom, A., Freedman, R., Mulkins, M., Bhakta, S., McCarley, D., Wiesent, L., Wong, B., Jarnagin, K., and Handel, T. (1998) *J. Biol. Chem. 273*, 33157−65.
71. Chakravarty, L., Rogers, L., Quach, T., Breckenridge, S., and Kolattukudy, P. E. (1998) *J. Biol. Chem. 273*, 29641−7.
72. Chen, Z., Zhang, X., Gonnella, N. C., Pellas, T. C., Boyar, W. C., and Ni, F. (1998) *J. Biol. Chem. 273*, 10411−9.
73. Hammond, M. E., Shyamala, V., Siani, M. A., Gallegos, C. A., Feucht, P. H., Abbott, J., Lapointe, G. R., Moghadam, M., Khoja, H., Zakel, J., and Tekamp-Olson, P. (1996) *J. Biol. Chem. 271*, 8228−35.
74. Schraufstatter, I. U., Ma, M., Oades, Z. G., Barritt, D. S., and Cochrane, C. G. (1995) *J. Biol. Chem. 270*, 10428−31.
75. Nicholls, A., Sharp, K. A., and Honig, B. (1991) *Proteins 11*, 281−96.

BI991029M